Chemical Science

ROYAL SOCIETY OF CHEMISTRY

EDGE ARTICLE

View Article Online
View Journal | View Issue

Cite this: *Chem. Sci.*, 2023, **14**, 4418

All publication charges for this article have been paid for by the Royal Society of Chemistry

Functional characterization, structural basis, and regio-selectivity control of a promiscuous flavonoid 7,4′-di-*O*-glycosyltransferase from *Ziziphus jujuba* var. *spinosa*†

Zi-Long Wang, ‡[a] Wanqing Wei,‡[b] Hai-Dong Wang,‡[a] Jia-Jing Zhou,[a] Hao-Tian Wang,[a] Kuan Chen,[a] Rong-Shen Wang,[a] Fu-Dong Li,[c] Xue Qiao,[a] Huan Zhou,*[d] Yong Liang*[e] and Min Ye*[a]

Received 25th November 2022
Accepted 29th March 2023

DOI: 10.1039/d2sc06504e

rsc.li/chemical-science

A highly efficient and promiscuous 7,4′-di-*O*-glycosyltransferase ZjOGT3 was discovered from the medicinal plant *Ziziphus jujuba* var. *spinosa*. ZjOGT3 could sequentially catalyse 4′- and 7-*O*-glycosylation of flavones to produce 7,4′-di-*O*-glycosides with obvious regio-selectivity. For 7,4′-dihydroxyl flavanones and 3-*O*-glycosylated 7,4′-dihydroxyl flavones, ZjOGT3 selectively catalyses 7-*O*-glycosylation. The crystal structure of ZjOGT3 was solved. Structural analysis, DFT calculations, MD simulations, and site-directed mutagenesis reveal that the regio-selectivity is mainly controlled by the enzyme microenvironment for 7,4′-dihydroxyl flavones and 3-*O*-glycosylated 7,4′-dihydroxyl flavones. For 7,4′-dihydroxyl flavanones, the selectivity is mainly controlled by intrinsic reactivity. ZjOGT3 is the first plant flavonoid 7,4′-di-*O*-glycosyltransferase with a crystal structure. This work could help understand the catalytic mechanisms of multi-site glycosyltransferases and provides an efficient approach to synthesise *O*-glycosides with medicinal potential.

Introduction

Glycosylation is an important post-modification biosynthetic reaction in plant secondary metabolism.[1] This type of reaction is generally catalyzed by uridine diphosphate (UDP)-dependent glycosyltransferases (UGTs).[2] Thus far, a huge family of glycosyltransferases (GTs) has been discovered from plants.[3] They provide powerful tools to prepare important bioactive glycosides, including schaftoside,[4] stevioside,[5] glycyrrhizin,[6] and ginsenosides.[7] Glycosylation of polyhydroxyphenolics by chemical synthesis is usually limited by poor regio- and stereoselectivity and protection and deprotection of unstable hydroxyl groups under severe conditions.[8] In contrast, GT-mediated glycosylation reactions take only one step and exhibit high catalytic efficiency.[9] However, many GTs suffer from poor selectivity, particularly regio-selectivity when multiple glycosylation sites are present.[3c,d,10]

Flavonoids represent a large class of polyphenols and are widely distributed in plants.[11] They possess a variety of bioactivities, including anti-inflammatory, antioxidative, anti-viral, antitumor, hepatoprotective, and cardio-cerebrovascular protective activities.[12] For example, diosmin and scutellarin are used as clinical drugs to treat lymphatic insufficiency and brain stroke in China, respectively. Flavonoids also contribute to plant tastes[13] and flower pigments.[14]

Thus far, more than 10 000 flavonoids have been reported.[11,15] Due to the common biosynthetic pathway, a large proportion of flavonoids possess two conserved hydroxyl groups at 7-OH and 4′-OH.[16] Although many GTs have been reported to catalyse 7- and 4′-*O*-glycosylation reactions, very few of them show high catalytic efficiency and high regio-selectivity.[17] F4′GT and F4′G7GT from *Nemophila menziesii* could catalyse stepwise 7,4′-*O*-glycosylation to form flavonoid 4′-*O*-glycosides and 7,4′-di-*O*-glycosides, respectively.[18] However, they could only accept a limited range of substrates.

Wild jujube (*Ziziphus jujuba* var. *spinosa*, Rhamnaceae family) is a medicinal plant native to China. Its seeds have been used as the

[a]*State Key Laboratory of Natural and Biomimetic Drugs, School of Pharmaceutical Sciences, Peking University, 38 Xueyuan Road, Beijing 100191, China. E-mail: yemin@bjmu.edu.cn*

[b]*State Key Laboratory of Food Science and Technology, Jiangnan University, Wuxi 214122, China*

[c]*Hefei National Laboratory for Physical Science at Microscale, School of Life Sciences, University of Science and Technology of China, Hefei 230036, China*

[d]*Shanghai Synchrotron Radiation Facility, Shanghai Advanced Research Institute, Chinese Academy of Sciences, 239 Zhangheng Road, Pudong District, Shanghai 201204, China. E-mail: zhouhuan@sari.ac.cn*

[e]*State Key Laboratory of Coordination Chemistry, Jiangsu Key Laboratory of Advanced Organic Materials, Chemistry and Biomedicine Innovation Centre (ChemBIC), School of Chemistry and Chemical Engineering, Nanjing University, Nanjing 210023, China. E-mail: yongliang@nju.edu.cn*

† Electronic supplementary information (ESI) available: Details of experimental procedures, including molecular cloning, protein expression and purification, catalytic reaction analysis, product purification, structural characterisation, crystal structure and DFT calculations, LC/MS analysis, and NMR and ESI-MS spectra. See DOI: https://doi.org/10.1039/d2sc06504e

‡ These authors contributed equally.

traditional Chinese medicine Suan-Zao-Ren for a long time to treat anxiety and depression.[19] This plant contains abundant flavonoid 4′-*O*-glycosides.

In this work, we report a regio-selective flavonoid 7,4′-di-*O*-glycosyltransferase ZjOGT3 (UGT84A68) from *Z. Jujuba* var. *spinosa*. Mechanisms for its regio-selectivity were dissected by crystal structure analysis, density functional theory (DFT) calculations, molecular docking, molecular dynamics (MD) simulation, binding free energy calculations, and site-directed mutagenesis.

Results and discussion

Molecular cloning and functional characterization of ZjOGT3

Six transcriptome data sets of *Ziziphus jujuba* var. *spinosa* (SRR9721936, SRR9721937, SRR9721938, SRR9721939, SRR9721941, and SRR9721944) were downloaded from the Sequence Read Archive (SRA) database of NCBI, and clean reads were *de novo* assembled using the Trinity program (K-mer = 31) with default parameters. Several reported UDP-glycosyltransferase genes were selected as query sequences (Table S1†). By using local BLAST search, 24 putative full-length GT genes (ZjOGT1-24) were discovered.[20] After heterologous expression and functional characterization, ZjOGT3 was identified as a flavone 7,4′-di-*O*-glycosyltransferase. The cDNA sequence of ZjOGT3 contains an open reading frame (ORF) of 1440 bp encoding 479 amino acids (Table S2 and Fig. S1†). It was named UGT84A68 (accession number: OQ603459) by the UGT Nomenclature Committee.

The catalytic function of ZjOGT3 was characterized using kumatakenin B (**1**, 7,4′-dihydroxy flavone) as a sugar acceptor and uridine 5′-diphosphate glucose (UDP-Glc) as a sugar donor. The enzymatic reaction system contained 25 μg purified protein, 0.1 mM substrate (**1**), and 0.5 mM UDP-Glc in 100 μL of 50 mM NaH_2PO_4–Na_2HPO_4 buffer (pH 8.0). After co-incubation at 37 °C for 8 h, the products were analyzed by liquid chromatography coupled with mass spectrometry (LC/MS) (Table S3†). ZjOGT3 could completely convert **1** into a more polar product **1b** (Fig. 1A and B). The mass spectrum of **1b** showed an $[M\text{-}H+HCOOH]^-$ ion at *m*/*z* 623, which was 370 amu greater (2Glc + HCOOH) than **1**, indicating **1b** as a di-*O*-glucoside. The structure of **1b** was fully identified as 7,4′-di-*O*-glycoside flavone by comparing with an authentic reference standard.[10a] However, after 15 min of co-incubation, **1** was converted into **1a** as the main product, which was identified as kumatakenin B 4′-*O*-glucoside (Fig. 1B and S2†). These results indicated that ZjOGT3 could catalyse glucosylation of **1** at 4′- and 7-OH consecutively. Kumatakenin B 7-*O*-glucoside was never observed as a main product.

The biochemical properties of recombinant ZjOGT3 were further investigated using **1** and UDP-Glc as substrates. ZjOGT3 showed its maximum activity at pH 8.0 (50 mM NaH_2PO_4–Na_2HPO_4 buffer) and 45 °C and was independent of divalent cations (Fig. S3†). The apparent kinetic parameters for **1** and **1a** with saturated UDP-Glc were measured (Fig. S4†). The K_m value for **1** and **1a** was 15.57 μM and 197.70 μM, respectively. The catalytic efficiency (k_{cat}/K_m) for the 4′-*O*-glycosylation of **1** (0.010462 $\mu M^{-1}\ s^{-1}$) was around 53 times higher than that for 7-*O*-glycosylation of **1a** (0.0002014 $\mu M^{-1}\ s^{-1}$). Thus, the second step was rate-limiting to form **1b**.

Substrate promiscuity and synthetic applicability of ZjOGT3

To explore the substrate specificity of ZjOGT3, 34 flavonoids were screened by enzymatic assay using UDP-Glc as the sugar donor (Fig. 2). These substrates included 7,4′-dihydroxy flavones (**1–9**), 7,4′-dihydroxy flavanones (**10–11**), 3-*O*-glycosylated 7,4′-dihydroxy flavones (**12–17**), 7 or 4′ monohydroxy flavones (**18–28**), isoflavones (**29–31**), isoflavans (**32**), isoflavone glycoside (**33**), and chalone (**34**). LC/MS analysis revealed that ZjOGT3 could catalyse glucosylation

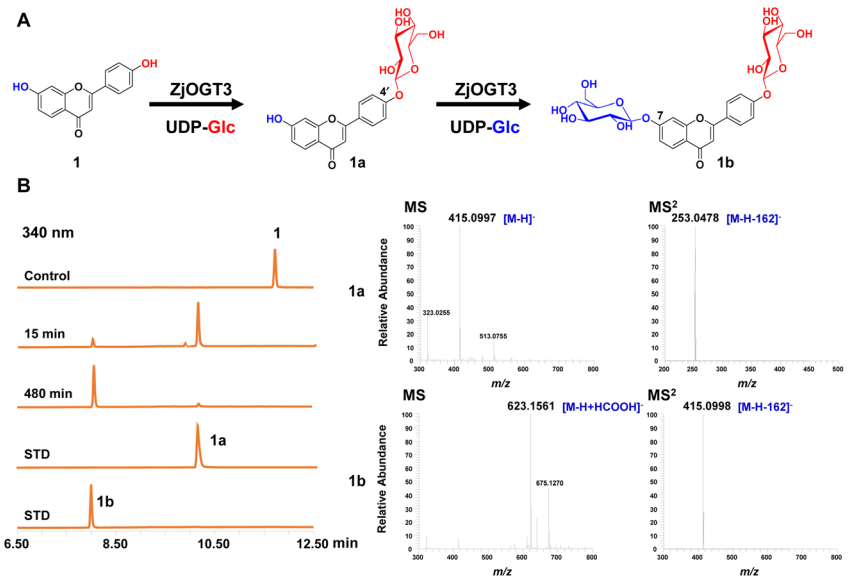

Fig. 1 7,4′-Di-*O*-glucosylation of kumatakenin B (**1**) catalysed by recombinant ZjOGT3. (A) Two-step glucosylation of **1** to produce **1a** and **1b**. (B) LC/MS analysis of the enzymatic reaction products after 15 or 480 min of co-incubation. The (−)-ESI-MS and MS/MS spectra of **1a** and **1b** are shown. The HPLC chromatograms were recorded at 340 nm. STD, reference standard.

of all 34 substrates. The glucosylated products were characterized by the diagnostic fragment ions $[M\text{-}H\text{-}162]^-$ in the MS/MS spectra (Fig. S5–S38†). Some of the products were purified and fully identified by NMR spectroscopy or by comparing with reference standards.

Interestingly, ZjOGT3 could efficiently glycosylate **1–9** (Type 1) to generate one mono-*O*-glycoside and one di-*O*-glycoside. The di-*O*-glycoside was usually the major product (Fig. S5–S13†). Furthermore, we fully identified **1a**, **2a**, **3a**, **4a** and **7a** as 4′-mono-*O*-glycosides and **1b**, **2b**, **3b**, **4b** and **7b** as 7,4′-di-*O*-glycosides by NMR spectroscopic analyses and standards (Fig. S39–S53†). For **10–11** which are flavanones with 7- and 4′-OH (Type 2), ZjOGT3 could only produce 7-mono-*O*-glycosides (**10a** and **11a**) (Fig. S14–S21 and S54–S60†). Similarly, for 3-*O*-glycosylated 7,4′-dihydroxy flavones with 7- and 4′-OH (**12–17**, Type 3), ZjOGT3 also could only produce 7-*O*-glycosides, and the structure of **12a** was fully identified (Fig. S61–S64†). For Type 4 flavonoids which contain either one 7-OH or one 4′-OH (**18–28**), ZjOGT3 could produce the corresponding 7 or 4′-*O*-glucosides (Fig. S22–S32 and S65–S79†). Moreover, ZjOGT3 could also accept isoflavones, isoflavans, isoflavone glycosides and

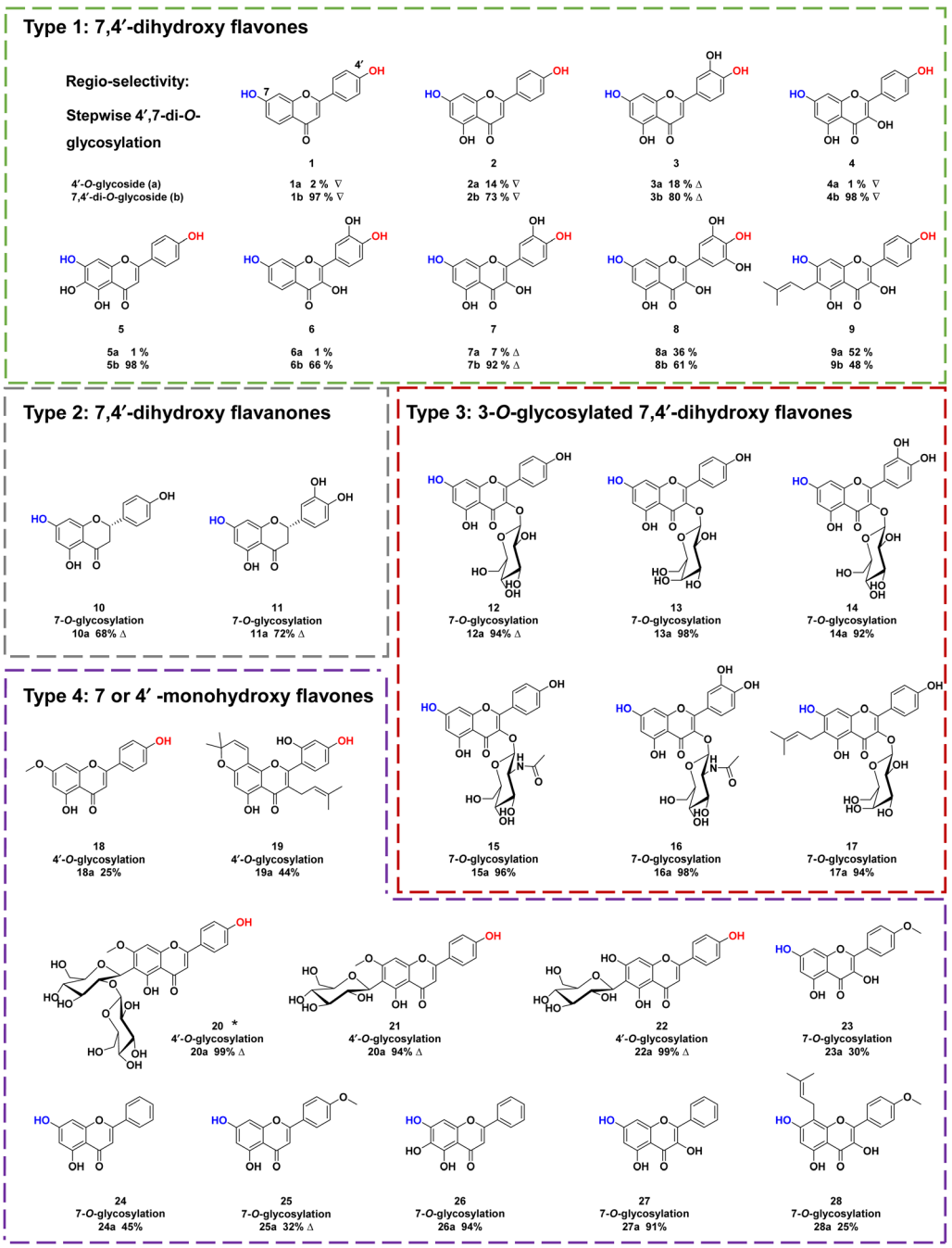

Fig. 2 Substrate promiscuity of ZjOGT3. Δ indicates that the products were purified and their structures were confirmed by NMR spectroscopy; ∇ indicates that the products were confirmed by comparing with reference standards. * represents new compounds.

chalcones (**29–34**) as substrates (Fig. S33–S38†). The above results indicate that the C2–C3 double bond and 3-*O*-glucosyl substitution could remarkably alter the regio-selectivity of ZjOGT3. A 6-*C*-glucosyl substituent could also inhibit 7-*O*-glycosylation, as ZjOGT3 only catalysed 4′-*O*-glycosylation of **22**.

To explore the sugar donor promiscuity of ZjOGT3, we tested six other sugar donors, including UDP-galactose (UDP-Gal), UDP-xylose (UDP-Xyl), UDP-arabinose (UDP-Ara), UDP-glucuronic acid (UDP-GlcA), UDP-*N*-acetylglucosamine (UDP-GlcNAc), and UDP-rhamnose (UDP-Rha). Compound **1** was used as the substrate. The results demonstrated that ZjOGT3 could accept UDP-Glc, UDP-Xyl, UDP-Ara, and UDP-GlcNAc. Among these four positive sugar donors, ZjOGT3 produced di-*O*-glycoside as the major product for UDP-Glc. While the conversion rate for UDP-Xyl was almost 100%, mono-*O*-glycoside was the major product. The conversion rates for UDP-Ara and UDP-GlcNAc were relatively low (Fig. S80†).

Crystal structure of the ZjOGT3/UDP complex

Although the crystal structures of many plant glycosyltransferases have been reported, little is known about catalytic mechanisms for stepwise di-*O*-glycosylation and regio-selectivity.[5,21] In this work, we obtained the crystal structure of ZjOGT3 in complex with UDP at 2.50 Å resolution (PDB: 8INH) (Fig. 3, S81 and Table S4†). To our knowledge, ZjOGT3 is the first plant flavonoid di-*O*-glycosyltransferase with a crystal structure. ZjOGT3 adopts a canonical GT-B fold consisting of two Rossmann-like β/α/β domains that face each other and are separated by a deep cleft.[9] The N-terminal domain (NTD, residues 1–246 and 443–470) and the C-terminal domain (CTD, residues 247–442) are responsible primarily for sugar acceptor and sugar donor binding, respectively (Fig. 3B and C). We made a lot of efforts to obtain the crystal structure in complex with the sugar acceptor by optimizing protein/ligand concentrations, pH values, temperatures, and precipitant concentrations, but we were not successful.

Catalytic mechanisms for the regio-selectivity

To reveal the catalytic mechanisms for regio-selectivity of ZjOGT3, we conducted DFT calculations on the glycosylation of substrate **2** (Fig. 4A and Table S5†). The 7-OH of **2** is in a deprotonated form in the pH 8.0 buffer, since its pK_a was estimated to be around 7.[22] In the presence of HPO_4^{2-} ions,[23] deprotonation of **2** is spontaneous and computed to be exergonic by 13.0 and 11.5 kcal mol^{-1} in water at 4′-OH and 7-OH, respectively (Fig. 4A), suggesting that **2** is deprotonated without enzyme catalysis under the experimental conditions. This is remarkably different from reported glycosyltransferase mechanisms, where deprotonation of a hydroxyl group activated by a histidine (His) residue is critical to initiate GT-mediated glycosylation.[3,9] Subsequently, the anionic intermediate performs nucleophilic attack *via* a S_N2-like transition state and generates the corresponding *O*-glucoside. The overall glycosylation barrier for 4′-OH in **2** (*via* **TS2-b**, 26.8 kcal mol^{-1}) is 0.9 kcal mol^{-1} higher than that for 7-OH (*via* **TS2-a**, 25.9 kcal mol^{-1}) (Fig. 4A), indicating that the innate nucleophilicity of the oxyanion at the 4′-position is not more favored than that of 7-OH. This result is not, however, consistent with the observed 4′-*O*-glucosylation catalysed by ZjOGT3. Therefore, the enzyme microenvironment is also a critical factor affecting the regio-selectivity of ZjOGT3.

Subsequently, we employed the combination of molecular docking,[24] MD simulations,[25] and binding free energy calculations[26] to reveal the binding mechanisms of **2** in its two phenolate forms (**2-IMa**, the oxyanion at the 7-position; and **2-IMb**, the oxyanion at the 4′-position) into ZjOGT3. First, we constructed the binary complex configuration of ZjOGT3 in complex with UDP-Glc based on the crystal structure and selected a representative MD-equilibrated snapshot as the target receptor for molecular docking. Then, we docked **2-IMa** and **2-IMb** into the active site and identified catalytically active binding modes as initial configurations to perform MD simulations of the ternary complexes (Fig. S82†). **2-IMa** and **2-IMb** locate above UDP-Glc in a hydrophobic pocket constituted by F14, A16, L87, L199, I285 and F318 residues, defining a cavity in which acceptors with an aromatic group can be easily accommodated (Fig. 5A). Additionally, H19 stabilizes these two anionic intermediates by forming a hydrogen bond with the nucleophilic attacking phenolic anion. According to the DFT-optimized structures, we defined the active conformation (shown in the light green dotted rectangle) that would lead to the formation of *O*-glucoside as O–C1 distance ≤3.4 Å (the sum of van der Waals atomic radii of carbon and oxygen atoms[27]) and angle O–C1–O1 in the range of 140 ± 15°. Our calculations showed that the oxyanion at the 4′-position in **2-IMb** has a greater probability of being situated in a catalytically competent position and is more poised for nucleophilic attack than **2-IMa** (140/5000 for **2-IMb** *vs.* 84/5000 for **2-IMa**, Fig. 5B). To qualitatively rank the binding modes, we evaluated the binding free energies by the molecular mechanics generalized born surface area (MM/GBSA) method. The binding free energy of **2-IMb** is about 6.4 kcal mol^{-1} (Fig. 5A) lower

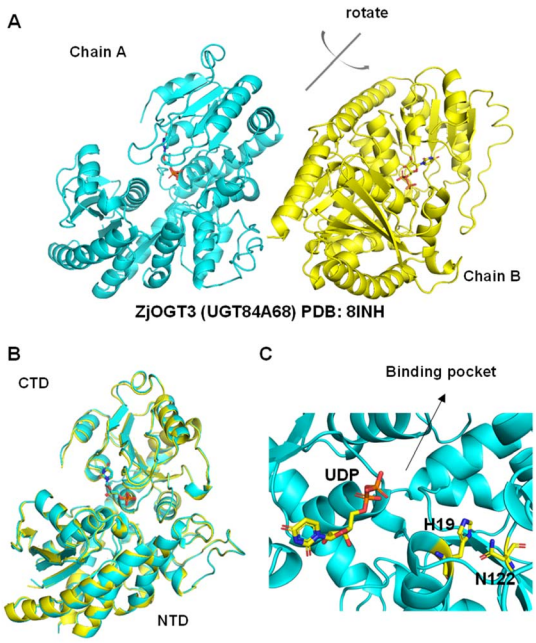

Fig. 3 Structural basis for the catalytic mechanisms of ZjOGT3. (A) The crystal structure of ZjOGT3 (PDB: 8INH); (B) superimposition of chain A and chain B of ZjOGT3; (C) a close view of the binding pocket.

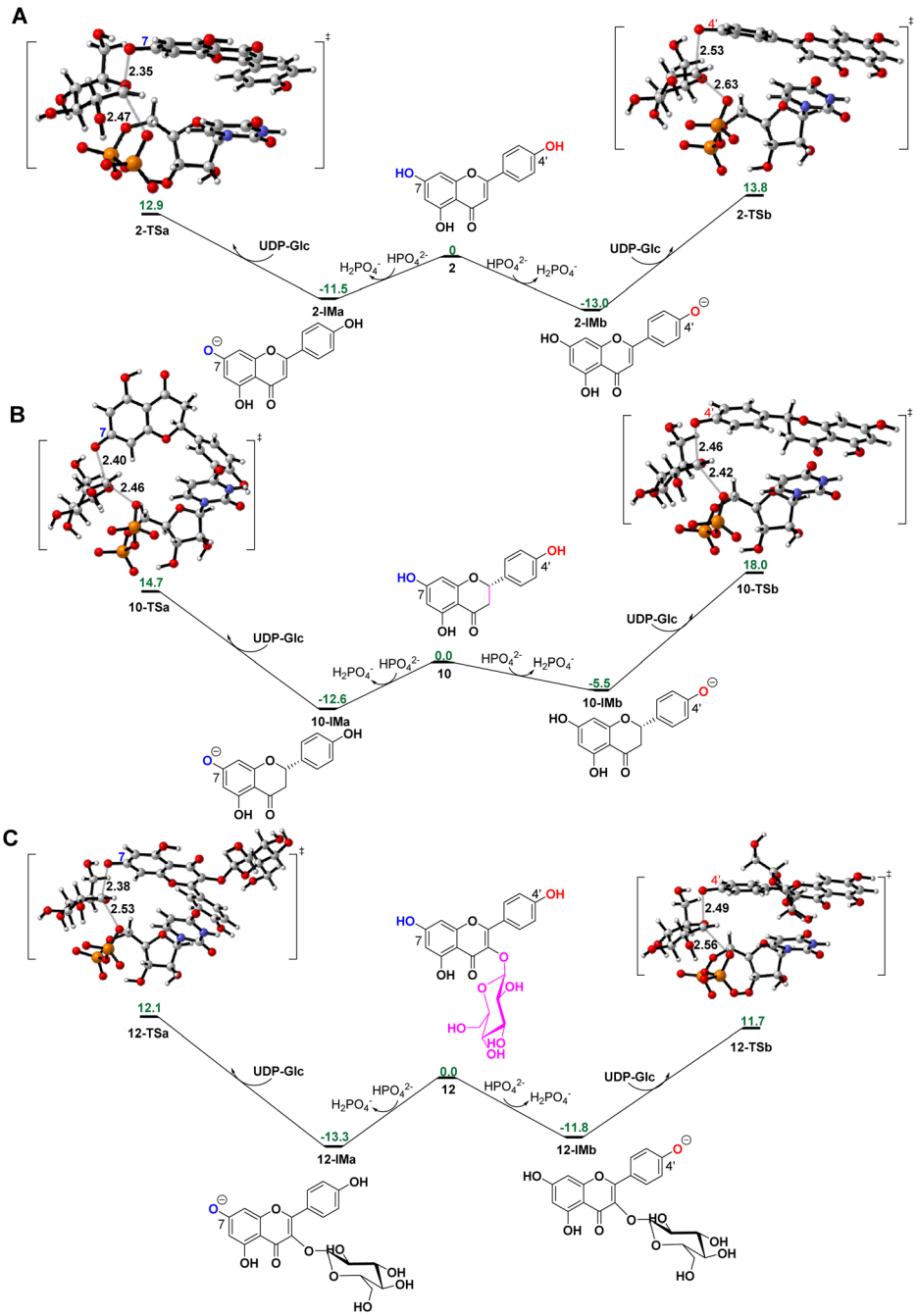

Fig. 4 Gibbs free energy profiles and DFT-optimized transition states for 7-*O*- and 4′-*O*-glucosylation of **2** (A), **10** (B), and **12** (C). Computed at the CPCM(water)-B3LYP-D3/6-311++G(2d,p)//CPCM(water)-B3LYP-D3/6-31+G(d,p) level of theory. Carbon, gray; hydrogen, white; oxygen, red; nitrogen, blue; phosphorus, orange. Distances are shown in Å.

than that of **2-IMa**, which is large enough to reverse the intrinsic reactivity. Taken together, 4′-*O*-glucoside has around 5.5 kcal mol^{-1} (6.4–0.9 kcal mol^{-1}) priority over 7-*O*-glucoside for substrate **2**, which is consistent with the experimental data. Overall, the regio-selectivity of **2**-*O*-glycosylation is mainly controlled by the enzymatic environment. Since H19 is closer to the nucleophilic attacking phenolic anion in **2-IMb** than **2-IMa**, there may be a stronger stabilizing effect of H19 in **2-IMb** (Fig. S83†). Per-residue contribution of binding energies of **2** in the two phenolate forms suggested that F14, A16, H19, H44, R84, R85, L87, F124, Q145, Y196, L199, I285, F318 and W382 may be key amino acids for substrate binding (Fig. S84†). As expected, alanine scanning mutagenesis for the above residues reduced the conversion rates to different extents (Fig. S85†). Interestingly, W382A and L199A mutants changed the catalytic sequence. They first catalyzed **2** to generate 7-*O*-glucoside and then 4′-*O*-glucosylation to generate di-*O*-glycoside. In these two mutants, we found that the oxyanion at the 4′-position in **2-IMb** has a lower probability of being situated in

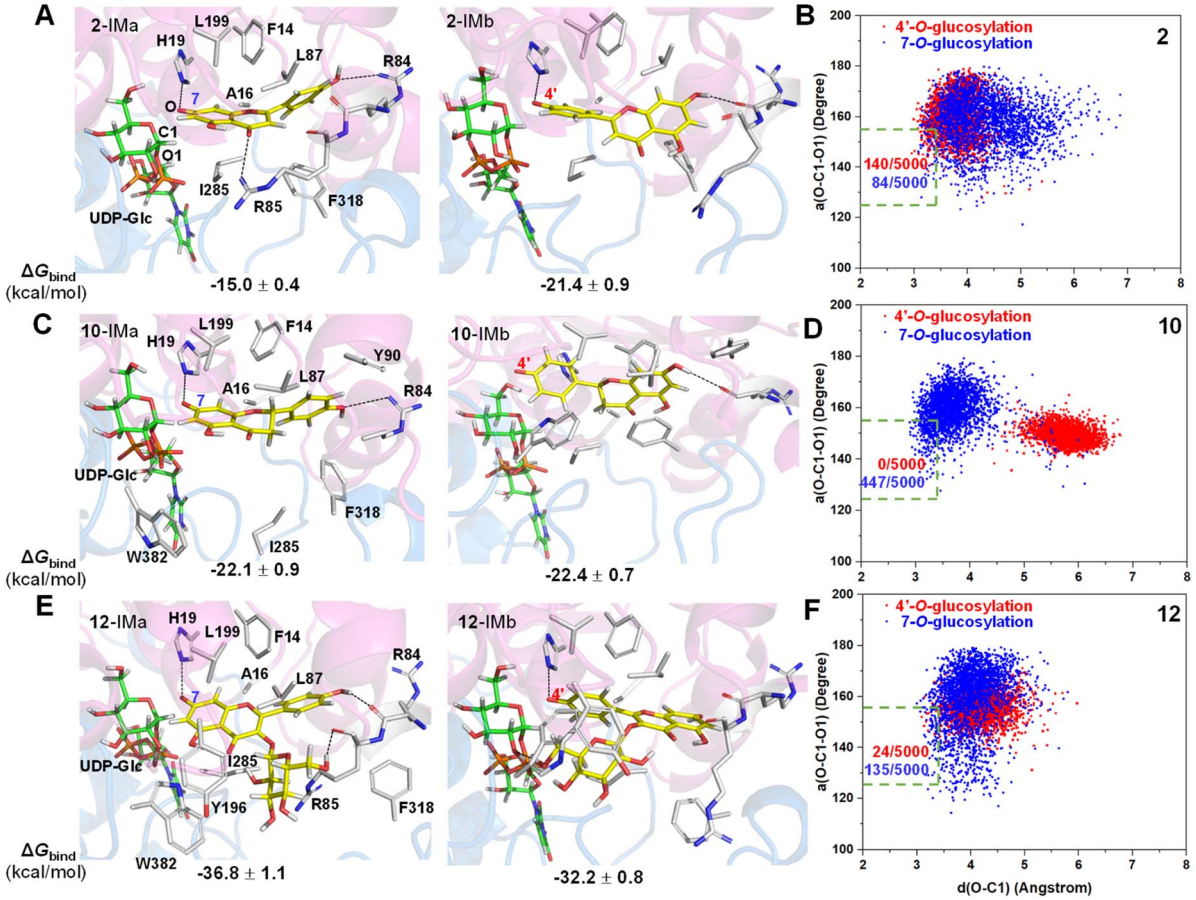

Fig. 5 Close-up views of representative ternary complex MD snapshots of the ZjOGT3 active site in complex with UDP-Glc and the anionic intermediates of acceptors **2**, **10** and **12** (A), (C) and (E), as well as the corresponding binding free energies calculated by MM/GBSA. (B), (D) and (F) MD plots for distances of the forming O–C bond *d*(O–C1) and angles between the forming O–C bond and the breaking C–O bond *a*(O–C1–O1) for the two anionic intermediates in the ternary complex.

a catalytically competent position and is less poised for nucleophilic attack than **2-IMa** by using molecular docking and MD simulations (Fig. S86 and S87†). In addition, the probability that the distance between the phenolic anion and the imidazole ring hydrogen atom of the H19 side chain is less than 2.0 Å in **2-IMa** is significantly higher than that in **2-IMb**. Overall, **2** should preferentially undergo 7-*O*-glycosylation in W382A and L199A mutants.

To further test our hypothesis, we studied the glycosylation of substrates **10** and **12**. Similarly, **10** and **12** would be deprotonated spontaneously under buffer solution conditions (Fig. 4B and C). For **10**, where the C2–C3 double bond is reduced, the conjugation effect of the oxyanion is significantly decreased, resulting in a remarkable increase in the total energy barrier, especially at 4′-OH (30.6 kcal mol^{-1} for **10-TSb** *vs.* 26.8 kcal mol^{-1} for **2-TSb**; 27.3 kcal mol^{-1} for **10-TSa** *vs.* 25.9 kcal mol^{-1} for **2-TSa**; Fig. 4B). Consistent with these calculations, only **10** underwent the 7-*O*-glucosylation reaction. Given that the binding free energies of the two anionic intermediates for compound **10** are almost the same (−22.1 *vs.* −22.4 kcal mol^{-1} in Fig. 5C), the site selectivity depends primarily on the innate reactivity. In addition, the enzyme microenvironment could further enhance the regio-selectivity (Fig. 5D).

For **12**, the introduction of a 3-*O*-glucosyl substituent has little effect on the intrinsic nucleophilicity because it is far from the reactive sites. The similar energy barriers for 7-*O*- and 4′-*O*-glycosylation also support our deduction (25.4 kcal mol^{-1} for **12-TSa** *vs.* 25.0 kcal mol^{-1} for **12-TSb**; Fig. 4C). In fact, ZjOGT3 exhibited high regio-selectivity toward 7-*O*-glycosylation for **12**. It is possible that the size and shape of the enzyme cavity make it easier to place **12-IMa** in a catalytically active conformation (135/5000 for **12-IMa** *vs.* 24/5000 for **12-IMb**; Fig. 5F). The favorable binding free energy (Δ 4.6 kcal mol^{-1}; Fig. 5E) makes 7-*O*-glucosylation the dominant reaction. Moreover, R84 and R85 could form two extra hydrogen bonds in **12-IMa**.

To interpret why only the free flavones or flavonols (**1–9**) could be catalysed to generate di-*O*-glycosides, we conducted DFT calculations and molecular docking (Fig. S88†). The energy barrier for 7-*O*-glycosylation of **2a** is 23.9 kcal mol^{-1}, and molecular docking and molecular dynamics simulations show that the conformation of **2a** in the active pocket is reasonable. Thus, 7-*O*-glycosylation of **2a** could occur. However, the docking

results show that **10a**, **12a** and **22a** have obvious steric hindrance (Fig. S89†). Thus, the second glycosylation is difficult to take place for **10**, **12**, and **22**.

Conclusions

In summary, we report an efficient flavonoid 7,4′-di-*O*-glycosyltransferase ZjOGT3 from *Z. jujuba* var. *spinosa*. ZjOGT3 has broad substrate promiscuity and could catalyse at least 34 flavonoids. The structures of 19 products were fully identified. For free 7,4′-hydroxy flavones, ZjOGT3 could catalyse 4′-*O*-glycosylation and 7-*O*-glycosylation sequentially to produce 7,4′-di-*O*-glycosides. For 7,4′-hydroxy flavanones and 3-*O*-glycosylated 7,4′-dihydroxyl flavones, ZjOGT3 selectively catalyses 7-*O*-glycosylation. For flavone-6-*C*-glycosides, however, ZjOGT3 only catalyses 4′-*O*-glycosylation. Furthermore, we solved the crystal structure of ZjOGT3 and interpreted mechanisms for the regio-selectivity by structural analysis, DFT calculations, molecular docking, MD simulation, MM/GBSA binding free energy calculations, and site-directed mutagenesis. For 7,4′-hydroxy flavones and 3-*O*-glycosylated 7,4′-dihydroxyl flavones such as **2** and **12**, the regio-selectivity is mainly controlled by the enzyme microenvironment, especially the binding orientation of substrates. For 7,4′-hydroxy flavanones such as **10**, the regio-selectivity is mainly controlled by the intrinsic reactivity. This work provides a highly efficient and regio-selective biocatalyst to prepare flavonoid 7,4′-*O*-glycosides and highlights regio-selectivity mechanisms based on structural analysis and theoretical calculations.

Data availability

Sequences for all the genes described in this paper and the crystal structure data have been submitted to the NCBI database and PDB, respectively. Accession number: ZjOGT3 (UGT84A68), OQ603459; ZjOGT2 (UGT84A67), OQ603460; ZjOGT6, OQ603461; ZjOGT10 (UGT71BJ1), OQ603462; ZjOGT13 (UGT72A17), OQ603463; ZjOGT15, OQ603464. PDB ID: ZjOGT3, 8INH. The other data needed to evaluate the conclusions are presented in the paper and/or the ESI.† Any additional data related to this paper may be requested from Min Ye (yemin@bjmu.edu.cn).

Author contributions

Min Ye and Zi-Long Wang conceived this study; Zi-Long Wang and Hai-Dong Wang conducted major investigations; Wanqing Wei and Yong Liang contributed to theoretical calculations; Huan Zhou and Fu-Dong Li supervised the crystallography experiments. Jia-Jing Zhou, Hao-Tian Wang, Kuan Chen, Rong-Shen Wang and Xue Qiao assisted with data acquisition; Min Ye, Zi-Long Wang and Wanqing Wei acquired funding; Zi-Long Wang and Wanqing Wei wrote the original draft; Min Ye and Yong Liang revised the manuscript.

Conflicts of interest

There are no conflicts to declare.

Acknowledgements

We thank the staff of the National Center for Protein Science Shanghai and Shanghai Synchrotron Radiation Facility, Shanghai, China, for assistance during data collection. We thank Dr Hong-Li Jia and Dr Fen Liu at State Key Laboratory of Natural and Biomimetic Drugs of Peking University for technical help in crystal and NMR experiments. This work was supported by the National Natural Science Foundation of China (Grant No. 81725023 to M. Y.), China National Postdoctoral Program for Innovation Talents (Grant No. BX20220022 to Z. L. W.), and Jiangsu Provincial Research Foundation for Basic Research (Grant No. BK20200335 to W. W.). We thank the High Performance Computing Center (HPCC) of Nanjing University for supporting the numerical calculations on its blade cluster system.

Notes and references

1 (*a*) D. Yi, T. Bayer, C. P. S. Badenhorst, S. Wu, M. Doerr, M. Hohne and U. T. Bornscheuer, *Chem. Soc. Rev.*, 2021, **50**, 8003–8049; (*b*) M. C. Tang, Y. Zou, K. Watanabe, C. T. Walsh and Y. Tang, *Chem. Rev.*, 2017, **117**, 5226–5333; (*c*) W. J. C. de Bruijn, M. Levisson, J. Beekwilder, W. J. H. van Berkel and J. P. Vincken, *Trends Biotechnol.*, 2020, **38**, 917–934.

2 Y. Q. Liu, Q. Wang, X. N. Liu, J. Cheng, L. Zhang, H. Y. Chu, R. Y. Wang, H. R. Li, H. Chang, N. Ahmed, Z. H. Wang, X. P. Liao and H. F. Jiang, *Mol. Plant*, 2023, DOI: **10.1016/j.molp.2023.01.003**.

3 (*a*) N. Putkaradze, D. Teze, F. Fredslund and D. H. Welner, *Nat. Prod. Rep.*, 2021, **38**, 432–443; (*b*) Y. Q. Zhang, M. Zhang, Z. L. Wang, X. Qiao and M. Ye, *Biotechnol. Adv.*, 2022, **60**, 108030; (*c*) E. Kurze, M. Wust, J. R. Liao, K. McGraphery, T. Hoffmann, C. K. Song and W. Schwab, *Nat. Prod. Rep.*, 2022, **39**, 389–409; (*d*) U. M. Vasudevan and E. Y. Lee, *Biotechnol. Adv.*, 2020, **41**, 107550.

4 Z. L. Wang, H. M. Gao, S. Wang, M. Zhang, K. Chen, Y. Q. Zhang, H. D. Wang, B. Y. Han, L. L. Xu, T. Q. Song, C. H. Yun, X. Qiao and M. Ye, *Proc. Natl. Acad. Sci. U. S. A.*, 2020, **117**, 30816–30823.

5 (*a*) S. G. Lee, E. Salomon, O. Yu and J. M. Jez, *Proc. Natl. Acad. Sci. U. S. A.*, 2019, **116**, 13131–13136; (*b*) J. Zhang, M. Tang, Y. Chen, D. Ke, J. Zhou, X. Xu, W. Yang, J. He, H. Dong, Y. Wei, J. H. Naismith, Y. Lin, X. Zhu and W. Cheng, *Nat. Commun.*, 2021, **12**, 7030.

6 (*a*) A. Jozwiak, P. D. Sonawane, S. Panda, C. Garagounis, K. K. Papadopoulou, B. Abebie, H. Massalha, E. Almekias-Siegl, T. Scherf and A. Aharoni, *Nat. Chem. Biol.*, 2020, **16**, 740–748; (*b*) S. Y. Chung, H. Seki, Y. Fujisawa, Y. Shimoda, S. Hiraga, Y. Nomura, K. Saito, M. Ishimoto and T. Muranaka, *Nat. Commun.*, 2020, **11**, 5664.

7 (*a*) X. Yan, Y. Fan, W. Wei, P. Wang, Q. Liu, Y. Wei, L. Zhang, G. Zhao, J. Yue and Z. Zhou, *Cell Res.*, 2014, **24**, 770–773; (*b*) X. Li, Y. Wang, Z. Fan, Y. Wang, P. Wang, X. Yan and Z. Zhou, *Metab. Eng.*, 2021, **66**, 87–97.

8 M. Jager and A. J. Minnaard, *Chem. Commun.*, 2016, **52**, 656–664.
9 D. M. Liang, J. H. Liu, H. Wu, B. B. Wang, H. J. Zhu and J. J. Qiao, *Chem. Soc. Rev.*, 2015, **44**, 8350–8374.
10 (*a*) K. Chen, Z. M. Hu, W. Song, Z. L. Wang, J. B. He, X. M. Shi, Q. H. Cui, X. Qiao and M. Ye, *ACS Synth. Biol.*, 2019, **8**, 1858–1866; (*b*) K. B. Xie, R. D. Chen, J. H. Li, R. S. Wang, D. W. Chen, X. X. Dou and J. G. Dai, *Org. Lett.*, 2014, **16**, 4874–4877.
11 N. C. Veitch and R. J. Grayer, *Nat. Prod. Rep.*, 2011, **28**, 1626–1695.
12 J. B. Johnson, J. S. Mani, D. Broszczak, S. S. Prasad, C. P. Ekanayake, P. Strappe, P. Valeris and M. Naiker, *Phytother. Res.*, 2021, **35**, 3484–3508.
13 A. Frydman, O. Weisshaus, M. Bar-Peled, D. V. Huhman, L. W. Sumner, F. R. Marin, E. Lewinsohn, R. Fluhr, J. Gressel and Y. Eyal, *Plant J.*, 2004, **40**, 88–100.
14 (*a*) J. Ogata, Y. Kanno, Y. Itoh, H. Tsugawa and M. Suzuki, *Nature*, 2005, **435**, 757–758; (*b*) N. Noda, S. Yoshioka, S. Kishimoto, M. Nakayama, M. Douzono, Y. Tanaka and R. Aida, *Sci. Adv.*, 2017, **3**, e1602785.
15 (*a*) C. A. Williams and R. J. Grayer, *Nat. Prod. Rep.*, 2004, **21**, 539–573; (*b*) N. C. Veitch and R. J. Grayer, *Nat. Prod. Rep.*, 2008, **25**, 555–611.
16 Q. Zhao, Y. Zhang, G. Wang, L. Hill, J. K. Weng, X. Y. Chen, H. W. Xue and C. Martin, *Sci. Adv.*, 2016, **2**, e1501780.
17 (*a*) X. Liu, J. Cheng, G. Zhang, W. Ding, L. Duan, J. Yang, L. Kui, X. Cheng, J. Ruan, W. Fan, J. Chen, G. Long, Y. Zhao, J. Cai, W. Wang, Y. Ma, Y. Dong, S. Yang and H. Jiang, *Nat. Commun.*, 2018, **9**, 448; (*b*) Z. L. Wang, S. Wang, Z. Xu, M. W. Li, K. Chen, Y. Q. Zhang, Z. M. Hu, M. Zhang, Z. Y. Zhang, X. Qiao and M. Ye, *Org. Lett.*, 2019, **21**, 2241–2245; (*c*) Z. Wen, Z. M. Zhang, L. Zhong, J. Fan, M. Li, Y. Ma, Y. Zhou, W. Zhang, B. Guo, B. Chen and J. B. Wang, *ACS Catal.*, 2021, **11**, 14781–14790.
18 N. Okitsu, K. Matsui, M. Horikawa, K. Sugahara and Y. Tanaka, *Plant Cell Physiol.*, 2018, **59**, 2075–2085.
19 Y. Hua, X. X. Xu, S. Guo, H. Xie, H. Yan, X. F. Ma, Y. Niu and J. A. Duan, *J. Agric. Food Chem.*, 2022, **70**, 7871–7886.
20 Y. Q. Zhang, Z. L. Wang, Z. Chen, Z. T. Jin, A. Hasan, H. D. Wang, Y. W. Sun, X. Qiao, Y. Wang and M. Ye, *Chem. Commun.*, 2022, **58**, 2472–2475.
21 W. Huang, Y. He, R. Jiang, Z. Deng and F. Long, *ACS Catal.*, 2022, **12**, 2927–2937.
22 J. M. Cabot, E. Fuguet and M. Roses, *ACS Comb. Sci.*, 2014, **16**, 518–525.
23 (*a*) J. Shi, Y. Shi, J. C. Li, W. Wei, Y. Chen, P. Cheng, C. L. Liu, H. Zhang, R. Wu, B. Zhang, R. H. Jiao, S. Yu, Y. Liang, R. X. Tan and H. M. Ge, *J. Am. Chem. Soc.*, 2022, **144**, 7939–7948; (*b*) Y. Zhang, W. Zhao, Y. Chen, H. Yuan, H. Fang, S. Yao, C. Zhang, H. Xu, N. Li, Z. Guo, Q. Zhao, Y. Liang and W. He, *Nat. Commun.*, 2021, **12**, 2772.
24 S. Forli, R. Huey, M. E. Pique, M. F. Sanner, D. S. Goodsell and A. J. Olson, *Nat. Protoc.*, 2016, **11**, 905–919.
25 J. L. Klepeis, K. Lindorff-Larsen, R. O. Dror and D. E. Shaw, *Curr. Opin. Struct. Biol.*, 2009, **19**, 120–127.
26 P. A. Kollman, I. Massova, C. Reyes, B. Kuhn, S. H. Huo, L. Chong, M. Lee, T. Lee, Y. Duan, W. Wang, O. Donini, P. Cieplak, J. Srinivasan, D. A. Case and T. E. Cheatham, *Acc. Chem. Res.*, 2000, **33**, 889–897.
27 R. S. Rowland and R. Taylor, *J. Phys. Chem.*, 1996, **100**, 7384–7739.